RESEARCH PAPER

Effect of Different Sources of Radiation on the Characteristics of a Nano-Reinforced Polymeric Composite

Shaymaa Mohammed Fayyadh *, Sukaina Iskandar Yusuf, Maha M. Ibrahim

Department of Physics, College of Science, Tikrit University, Iraq

ARTICLE INFO

ABSTRACT

The fabrication of two composites using polymers (A) and (B) reinforced with nano-Alumina in ratios of (8,4)%, respectively, was the main focus of this study. To study the effect of both the irradiation time and the effectiveness of the radioactive sources, the manufactured samples were exposed to different periods (1,2,3) days when irradiated with sources of different efficacy (Sr^{90}), (Co^{60}). From the results of the examination via the atomic force microscope, it was found that the rate of distribution of the granular sizes and the nature of the surface of composite B was affected when the irradiation time was increased, as well as when using different sources of effectiveness, while composite A was very weakly affected by these conditions. It was also noted that the mechanical properties were affected by the irradiation parameters, where we notice a decrease in the hardness values and an improvement in the impact strength of both compounds when the source efficiency increases and the irradiation duration increases. The infrared spectrum gave a great role in the irradiation time, and it affected the appearance and disappearance of beams when irradiated with different sources on the two complexes. In the case of composite A, the CH band disappeared on the first day of irradiation with a source (Co^{60}). The rest of the bands appeared, but with varying intensity and frequency, with a slight displacement when the irradiation source changed. It was also noticed that there was a disappearance of the same beam for the composite (B) but on the third day of exposure to the (Sr^{90}) source. This disappearance or displacement of the beams indicates a kind of disintegration in the polymer chains. Increasing the percentage of nanopowder addition to the composite improves the mechanical.

How to cite this article

INTRODUCTİON

As well as known the different sources of radiation can affect the characteristics of a nano-reinforced polymeric composite by inducing chain scission, cross-linking, free radical formation, and affecting the dispersion and alignment of nanoparticles in the polymer matrix. The extent of these effects depends on the type and intensity of radiation used, as well as the type of polymer and nanoparticles used in the composite. The effect of different sources of radiation on the characteristics of a nano-reinforced polymeric composite can vary depending on the type and intensity of radiation used. 1) Ionizing radiation: Ionizing radiation can cause chain scission and cross-linking of polymer chains, leading to

* Corresponding Author Email: shymafaydh@tu.edu.iq

changes in the mechanical, thermal, and electrical properties of the composite. The degree of cross-linking depends on the radiation dose and the type of polymer used. In nano-reinforced polymeric composites, ionizing radiation can also affect the dispersion and alignment of nanoparticles in the polymer matrix. 2) UV radiation: UV radiation can cause photodegradation of polymers, leading to a decrease in mechanical strength and toughness. In nano-reinforced polymeric composites, UV radiation can also affect the stability and dispersion of nanoparticles in the polymer matrix. 3) Gamma radiation: Gamma radiation can cause similar effects as ionizing radiation, but with higher energy levels. It can also induce free radical formation, which can lead to chain scission and cross-linking of polymer chains. In nano-reinforced polymeric composites, gamma radiation can affect the dispersion and alignment of nanoparticles in the polymer matrix, as well as their surface chemistry. 4) X-ray radiation: X-ray radiation can also cause chain scission and cross-linking of polymer chains, but with lower energy levels than gamma radiation. It can also induce free radical formation and affect the surface chemistry of nanoparticles in the polymer matrix [1]. The impact of these rays varies depending on the internal chemical composition of the material as well as its physical and mechanical properties [2-8]. In general, when polymeric compounds are subjected to radiation, one or both of the following processes take place, causing a change in their characteristics [9–14]:

1- Crosslinking: This process causes molecules to join together, turning a solid material from flexible (ductile) to brittle.

2- Dissolution: In this process, ionization and irritation take place, and as a result, the primary polymer chain fissions. This process causes reduction of the molecular weight exponentially with radiation dose due to the disintegration.

In order to understand the effect of radiation on the molecules of the material, this study intends to investigate the effects of several radiation sources (Co^{60}, Sr^{90}) on a polymeric composite supported by different proportions of nano-Alumina and its mechanical, structural, and spectral features (IR spectrum).

MATERIALS AND METHODS

The manual casting procedure was utilized to construct the polymeric composite models, beginning by preparing the basic materials that would be used in their production.

Matrix Material

Unsaturated Polyester Resin manufactured by the Saudi Company (SIR) was used for this purpose. Polyester resins are thermosetting polymers and readily polymerize at ambient temperature. By adding specific reinforcing elements (fibers, wires, and powders), their characteristics can be enhanced [9]. Table 1 shows the characteristics of the unsaturated polyester used in the research mentioned by the manufacturer.

Table 1. Unsaturated Polyester Resin Mechanical Characteristics.

Shore hardness	Modulus of Elasticity (Mpa)	Heat Capacity (KJ.Kg, K^{-1})	Density (Kg/m^3)
70	4	1.2	1200

Table 2. Weight Ratios.

Composite Code	Al_2O_3	Polyester
A	8	92
B	4	96

Table 3. International Standards for Test Molds.

Test Types	Mold Dimensions (mm)	International Standards
Hardness	30×10×3	ASTM-D2240
Impact Strength	55×10×4	ISO-179

Reinforcement Materials

The first step: Alumina nanoparticles were used to reinforce the polymer with different proportions shown in Table 2. Whereas, the used alumina particles were prepared by (Allied High Tech) production company (USA), and the granular size was (50nm), density (3.97 gm/cm^3), and melting point (2323K).

The second step: Prepare the molds according to (ASTM) standards as in the following:

• Create glass molds for the examinations being studied with dimensions that adhere to international standards, as stated in Table 3.

• Clean the molds well

• Then, dry the molds well.

The molds are painted from the inner surface with Vaseline to ensure they do not stick when pouring.

The third step: Models can be manufactured after the molds are completed by following several steps: -

a) Starting with an addition ratio of 0.4%, mix the polymer with the reinforcement phase, then stir with a glass rod to ensure homogeneity. Next, add the reinforcing material using the weight ratios shown in Table 2, continuing the stirring process. Finally, add the hardener using an addition rate of (2%), and thoroughly mix for no more than three minutes to prevent rapid hardening before casting the mold. It is important to note that mixing all the materials with the hardener and accelerator at once runs the risk of causing violent decomposition.

b) The is then covered for 24 hours to harden.

c) To finish the production process, place the samples into an oven set at less than 100 °C for 24 hours to perform the treatment process. Then, the irradiation was carried out for all the polymeric samples under the same conditions so that the model was left at a distance of (10) cm in the air and for a while (1,2,3) day, equivalent to a radiation dose for the Co^{60} source of Gy / h (0.78,1.6,2.5), respectively. After that, the Sr^{90} source was used to irradiate the samples with the same time range and radiation doses Gy / h (1.7, 2.1, 3.4). The samples are prepared to undergo all testing after the irradiation process.

Characterization

To determine the success of the manufactured models, the following examinations must be carried out.

Atomic Force Microscopy- AFM

Using an atomic force microscope, the topography of the surfaces (AA 3000 SPM) is to be studied and examined. This technology uses cutting-edge, sophisticated technical procedures to enlarge the image of the material's surface. The AFM is characterized by the ability to magnify objects by up to (5×10^2–10^8) times and optical microscopy's high resolving power of (0.1–1.0) nm [15]–[18]. Since it gives us incredibly exact data on surface roughness and grain size, atomic force microscopy is typically employed to measure a variety of physical parameters [19]–[23].

Fourier Transform Infrared spectroscopy- FTIR

An infrared spectrophotometer of Japanese origin (the FT-IR In infrared spectrophotometer Shimadzu 8400) was used to record the spectra. To conduct the examination, a powder of a drug was mixed with the sample to be analyzed by IR (KBr). The powder is formed into discs, after which the examination is carried out with a range of (400–4000) cm^{-1}.

Mechanical Testing

Because polymers function in dual ways having great strength while also being prone to deformation and impacted by environmental factors, the mechanical characteristics are among the most crucial ones that help people understand models made from polymer-based materials. The mechanical characteristics of molecules are influenced in one way or another by strong and secondary bonds. The following are the key mechanical tests being researched [24-28].

Hardness Test (Brinell)

This is considered as one of the most fundamental mechanical tests, as hardness measures a material's resistance to scratching or penetration. The hardness of the created models was measured using the rebound method with a Swedish hardness tester that could be programmed. These are displayed on the device screen employed for reading the average hardness values [29].

Impact Strength Testing

The Impact Strength Testing shows the strength of polymeric materials by calculating the energy required to break the sample under stress and at high speeds. The following relationship can

express the Impact Strength [30].

Impact resistance = Energy required to break (KJ) / Cross-sectional area of the sample (m2)

An impact strength testing device manufactured by (Testing Machines INC, Amityville, New York) was used to conduct this test. The test was implemented at room temperature.

RESULTS AND DISCUSSION

You format your paper and save the content as a .doc/.docs file. Do not use tabs, and limit the use of one interval at the end of a paragraph. Do not add any kind of pagination anywhere in the paper. Please take note of the following items when proofreading spelling and grammar.

Effect of Irradiation on Atomic Force Microscopy

Figs. 1, 2, 3, and 4 depict the effects of radiation from both sources on the topography of the surface. When composite A was exposed to radiation from different sources, there was no difference in the effects on the rate of granular size distribution or the surface roughness, as depicted in Figs. 1 and 2. The effect of the (Sr^{90}) source on composite B was more substantial than the effect of the (Co^{60}) source on the same composite. Here, it was noticed that the roughness rate increased, while there was no discernible difference in the distribution of granular sizes after exposure to radiation from both sources as demonstrated in
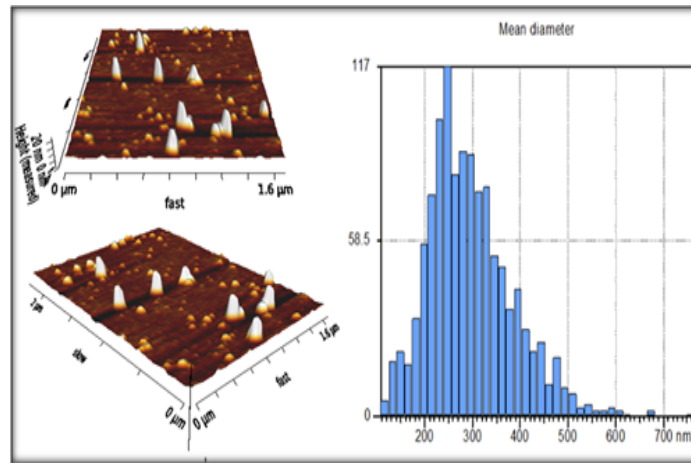

Fig. 1. AFM image of Composite (A) when irradiated with (Co^{60}) source for a period of (3 days).
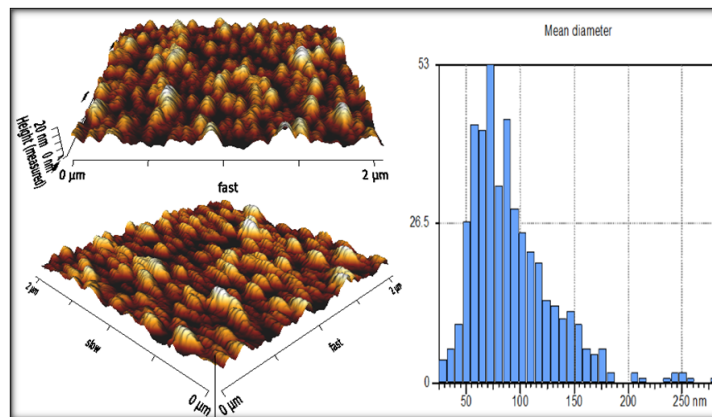

Fig. 2. (AFM) image of Composite (A) when irradiated with (Sr^{90}) source for a period of (3 days).
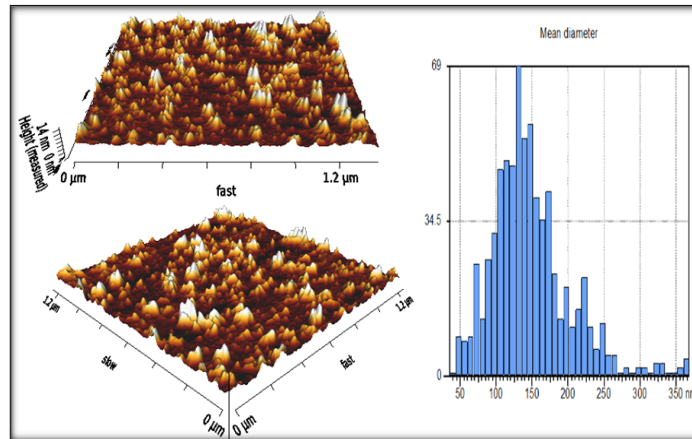
Fig. 3. (AFM) image of Compound (B) when irradiated with (Co^{60}) source for a period of (3days).
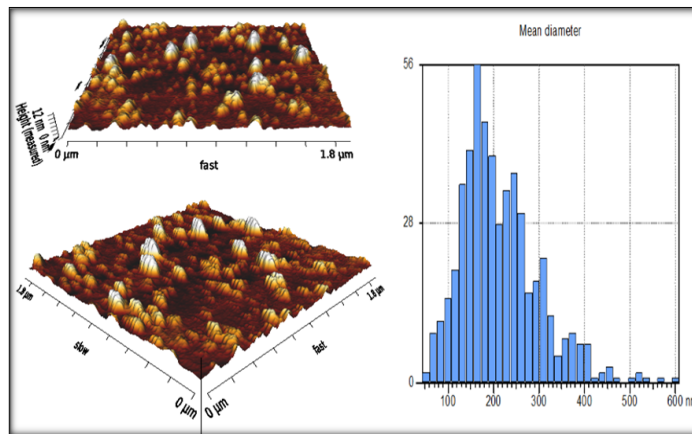

Fig. 4. (AFM) image of Composite (B) when irradiated with a source (Sr^{90}) for a period of (3 days).
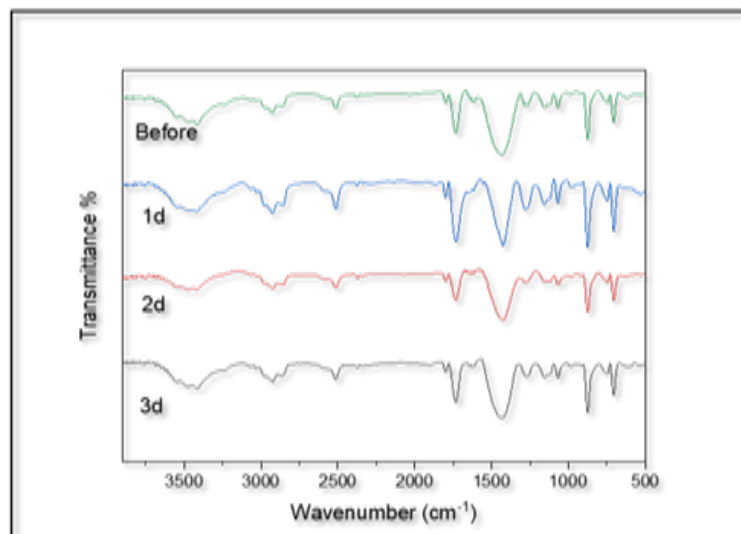

Fig. 5. IR spectrum of (A) by irradiating a source Co^{60}.

Figs. 3 and 4.

The Effect of Irradiation with Different sources on the Infrared Spectrum

The data values in Table 4 show that time has a negative effect on the flexibility and dissociation of the polymer, as was observed when composite (A) was subjected to a dose of radiation for a variable duration, such as 1, 2, or 3 days. It was noted that on the first day of exposure of the composite to the radiation source (Sr^{90}) that the (OH) group appeared at the frequency (3545-3414) cm^{-1} and the group (CH) appeared at the frequency (3064) cm^{-1}, while the exposure for one day to the source (Co^{60}) the (OH) group appeared at the frequency of (3545-3416) cm^{-1} and the (CH) group disappeared. This indicates dissociation of the polymer as shown in Figs 5 and 6. On the second day, when the polymer composite (A) was exposed to a source (Sr^{90}), it was noticed that the (OH) group appeared at the frequency (3547-3412) cm^{-1}, while when the polymer was exposed to a source (Co^{60}), this group appeared as (3545-3416) cm^{-1}. In terms of beam intensity, the remaining bundles were all very similar. The (OH) group appeared on the third day at a frequency (3545-3419) cm^{-1} when exposed to the source (Sr^{90}), whereas this group appeared at a frequency (3553-3414) cm^{-1} when exposed to
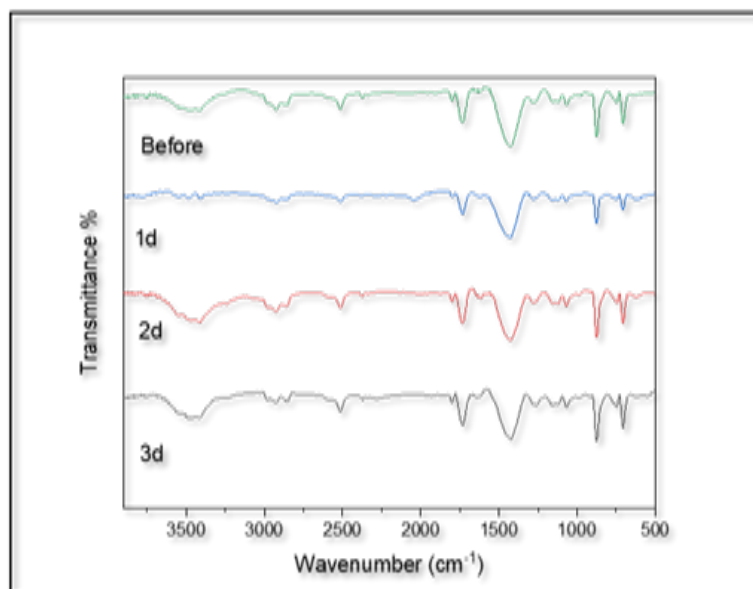

Fig. 6. IR spectrum of (A) by irradiating a source Sr^{90}.

Table 4. Locations of the essential absorption bands for the infrared spectra of the composite (A) when ex-posed to (Sr^{90}) and (Co^{60}) sources at different times.

Exposure time to (Sr^{90}) and (Co^{60}) sources/day		Beam locations /cm^{-1}				
		OH	C-H	C-C	C-O	C=O
before irradiation		3543-3417	2926-2854	----	1425	1732
1 day	irradiated source (Sr^{90})	3545-3414	3064-3028	3242	1425	1732-1614
	irradiator source (Co^{60})	3545-3416	3028-2856	3342-3246	1423	1732
2 day	irradiated source (Sr^{90})	3547-3412	2924	---	1429	1732
	irradiator source (Co^{60})	3545-3416	2924	3238	1427	1730
3 day	irradiated source (Sr^{90})	3545-3419	2976- 2858	----	1425	1732
	irradiator source (Co^{60})	3553-3414	2976-2856	----	1427	1732

the cobalt source. This difference in band intensity was due to the creation of free radicals, interaction of the hydrogen ion with oxygen radicals, and subsequent formation of peroxides.

Table 5. Locations of the essential absorption bands for the infrared spectra of the composite (B) when exposed to (Sr^{90}) and (Co^{60}) sources at different times.

| Exposure time to (Sr^{90}) and (Co^{60}) sources/day		Beam locations /cm^{-1}				
		OH	C-H	C-C	C-O	C=O
before irradiation		3545-3414	2978-2858	3236	1427	1732-1799
1 day	irradiated source (Sr^{90})	3554-3414	2924	3236	1427	1730-1790
	irradiator source (Co^{60})	3539-3417	3063-3028	3286- 3242	1438-1431	1732- 1799
2 day	irradiated source (Sr^{90})	3545- 3419	3063-3028	3246	1427	1732-1799
	irradiator source (Co^{60})	3556-3417	2926	----	1429	1732-1799
3 day	irradiated source (Sr^{90})	3545-3414	3063-3028	3242	1427	3545-3414
	irradiator source (Co^{60})	3400	2922	---	---	3400
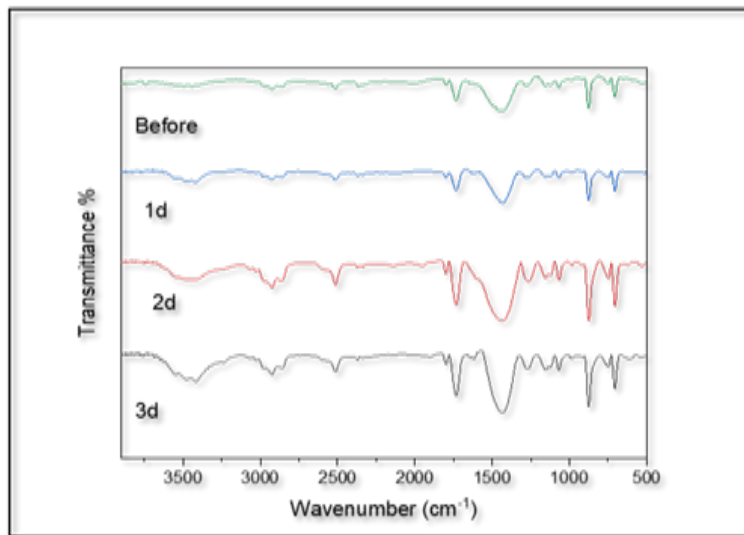
Fig. 7. IR spectrum of (B) by irradiating a source Co^{60}.
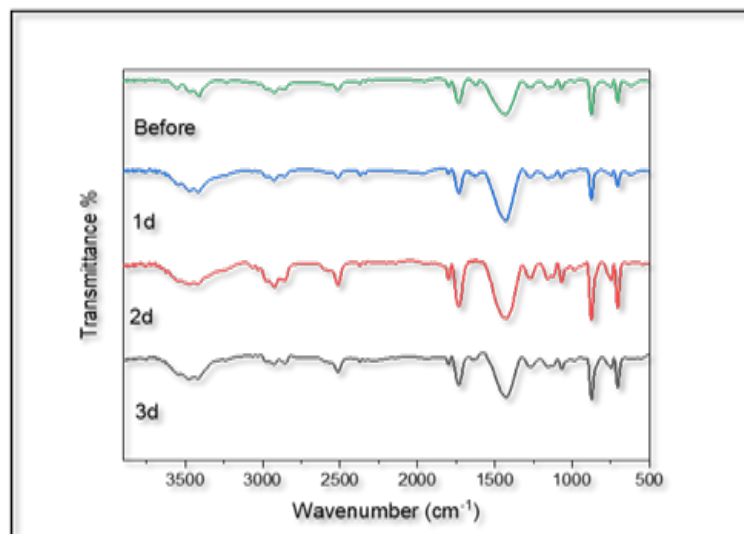

Fig. 8. IR spectrum of (B) by irradiating a source Sr^{90}.

According to Table 5, the dissociation process of the polymer composite (B) after exposure to both of the investigated sources differs noticeably. The appearance of the (CH) group as depicted in Figs. 7 and 8 as a result of the hydrogen ion's dissociation and its association with the oxygen free radical, causes the polymer to break down. This is the same as what occurred when exposed to a cobalt source, but with different beam intensities. The key findings on the second day of exposure to both sources were the appearance of a group (CH) at the frequency (3063-3028) cm^{-1} when exposed to a source (Sr^{90}), and the appearance of a group (CH) at the frequency (3063-3028) cm^{-1} when exposed to a source (Sr^{90}) for the group (CH).

Effect of irradiation with different sources on the hardness

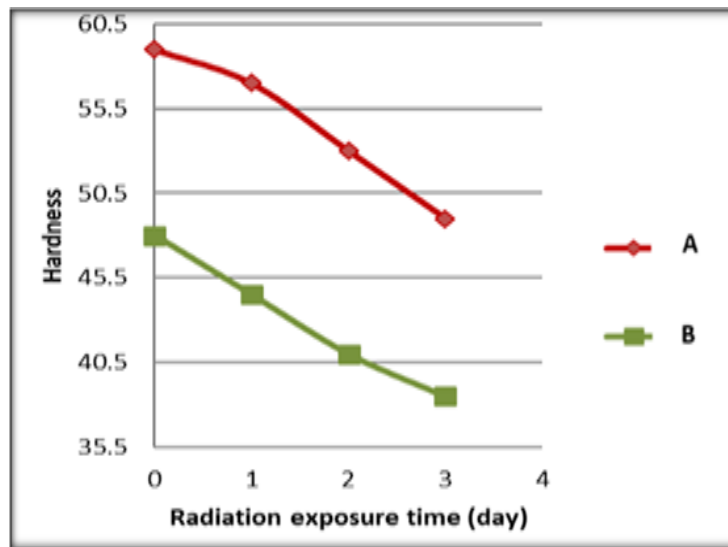Figs. 9 and 10 which show how irradiation with various sources affects the behavior of hardness

Fig. 9. Hardness when irradiating composites, A and B with a source (Co^{60}) for different periods.
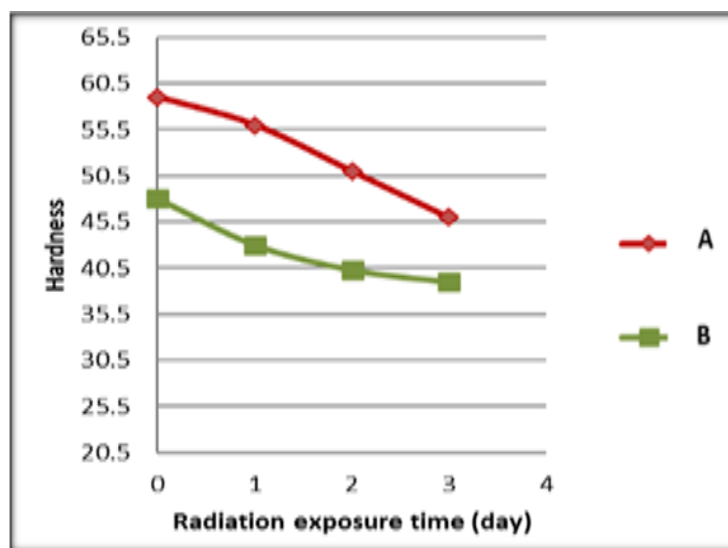

Fig. 10. Hardness when irradiating composites, A and B with a source (Sr^{90}) for different periods.

also demonstrate a decrease in hardness values for both composites when the exposure time is extended at irradiation with (Sr^{90}) and (Co^{60}) sources. This can be explained by the fact that on the first day of exposure, the bonds between the molecules of the composite materials (A, B) were under tension, which causes an interpretation of the movement of these molecules. As a result, on the third day of exposure, the composite material was complicated and had high hardness values relative to the hardness of the models. The complicated material (dissolution of the polymeric chains) is caused by a decrease in the bonding forces between the molecules.

Effect of irradiation time on impact strength

The properties of the composites (A) and (B) are significantly impacted by exposure duration following irradiation with both sources, as illustrated in Figs. 11 and 12. Yet, the Impact (Sr^{90}) source had the most notable impact because it was consistently more effective than the cobalt source.
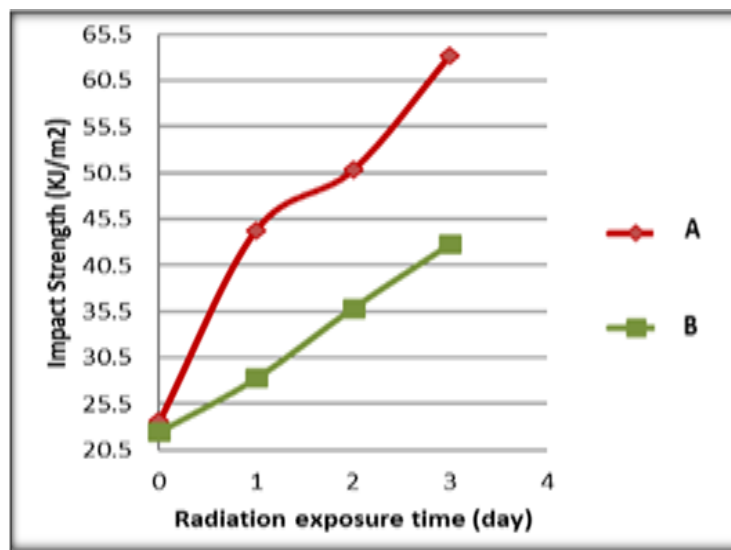

Fig. 11. Impact Strength when irradiating composites, A and B with a source (Co^{60}) for different periods.
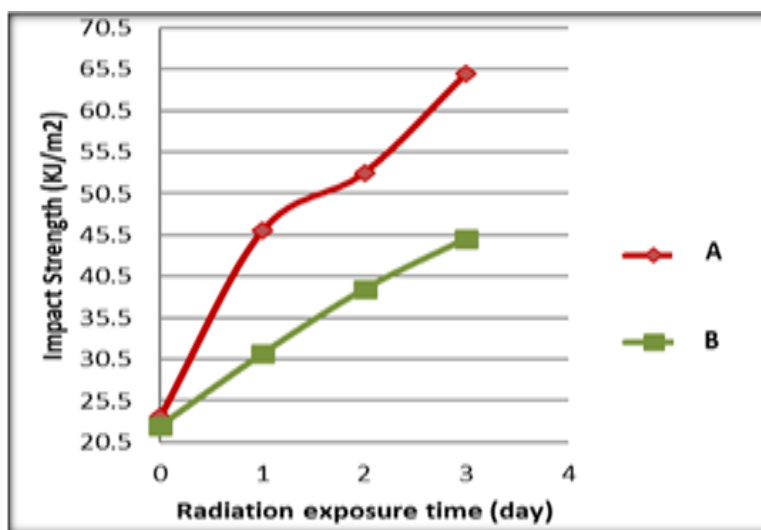

Fig. 12. Impact Strength when irradiating composites, A and B with a source (Sr^{90}) for different periods.

As a result, it was observed that a given chemical can behave either as a material with great strength or as a malleable material, depending on the external factors influencing it. It was found that when exposed to both sources, a material that is brittle on day one may behave as a high-strength material that may bend plastically on day three. This is due to the fact that the breaking energy increases This agrees with the researcher [31].

CONCLUSION

1- All composites' roughness and particle size distribution change as the radioactive source's potency increases.

2- For varied irradiation durations of polymer-based composites, the infrared spectrum was changed by the irradiation, which resulted in the disappearance of the (CH) beam when exposed to a source of weak activity, such as (Co^{60}), as opposed a source of (Sr^{90}), which is highly effective.

3- When exposed to highly effective sources and with an increase in exposure time, the impact resistance of the composite improves and its hardness values decrease.

4- Increasing the percentage of nano powder addition to the composite improves the mechanical

Acknowledgments

CONFLICT OF INTEREST

The authors declare that there is no conflict of interests regarding the publication of this manuscript.

REFERENCES

1. Chen J, Zhu Y, Guo Z, Nasibulin AG. Recent Progress on Thermo-electrical Properties of Conductive Polymer Composites and Their Application in Temperature Sensors. Engineered Science. 2020.
2. Shi Z, Zou C, Zhou F, Zhao J. Analysis of the Mechanical Properties and Damage Mechanism of Carbon Fiber/Epoxy Composites under UV Aging. Materials. 2022;15(8):2919.
3. Deep N, Mishra P. Evaluation of mechanical properties of functionalized carbon nanotube reinforced PMMA polymer nanocomposite. Karbala International Journal of Modern Science. 2018;4(2):207-215.
4. Al-Hadidy AI. Effect of laboratory aging on moisture susceptibility and resilient modulus of asphalt concrete mixes containing PE and PP polymers. Karbala International Journal of Modern Science. 2018;4(4):377-381.
5. Moezzi M, Yekrang J, Ghane M, Hatami M. The effects of UV degradation on the physical, thermal, and morphological properties of industrial nylon 66 conveyor belt fabrics. J Ind Text. 2019;50(2):240-260.
6. Mast B, Cambriani A, Douvalis AP, Pontikes Y, Schroeyers W, Vandoren B, Schreurs S. The effect of high dose rate gamma irradiation on the curing of CaO-FexOy-SiO2 slag based inorganic polymers: Mechanical and microstructural analysis. J Nucl Mater. 2020;539:152237.
7. Jabbar SA, Farid SBH. Replacement of steel rebars by GFRP rebars in the concrete structures. Karbala International Journal of Modern Science. 2018;4(2):216-227.
8. Acher L, de Noirfontaine M-N, Chartier D, Gorse – Pomonti D, Courtial M, Tusseau-Nenez S, et al. H$_2$ production under gamma irradiation of a calcium aluminate cement: An experimental study on both cement pastes and its stable hydrates. Radiat Phys Chem. 2021;189:109689.
9. Nihad Abed F, Mohammed Fayyadh S, Muhammed Awsaj E. Study the effect of reinforcement material in particles on the properties of unsaturated polyester. Materials Today: Proceedings. 2022;49:2949-2954.
10. Mahdi Salih W. Preparation and studying of some properties of polymer blend reinforced by natural powder. Materials Today: Proceedings. 2021;42:2202-2208.
11. Chayad FA, Jabur AR, Jalal NM. Effect of MWCNT addition on improving the electrical conductivity and activation energy of electrospun nylon films. Karbala International Journal of Modern Science. 2015;1(4):187-193.
12. Bakar SSS, Foong KM, Halif NA, Yahud S. Effect of solution concentration and applied voltage on electrospun polyacrylonitrile fibers. IOP Conference Series: Materials Science and Engineering. 2019;701(1):012018.
13. Balan GS, Krishnan AM, Saravanavel S, Ravichandran M. Investigation of hardness characteristics of waste plastics and egg shell powder reinforced polymer composite by stirring route. Materials Today: Proceedings. 2020;33:4090-4093.
14. Chartier D, Sanchez-Canet J, Bessette L, Esnouf S, Renault JP. Influence of formulation parameters of cement based materials towards gas production under gamma irradiation. J Nucl Mater. 2018;511:183-190.
15. Etcheverry LP, Flores WH, Silva DLd, Moreira EC. Annealing Effects on the Structural and Optical Properties of ZnO Nanostructures. Materials Research. 2018;21(2).
16. Mallika AN, Reddy AR, Reddy KV. Annealing effects on the structural and optical properties of ZnO nanoparticles with PVA and CA as chelating agents. Journal of Advanced Ceramics. 2015;4(2):123-129.
17. Mahan HM, Farhan MM, Shaalan TG. Studying Some Mechanical Properties of River Shell Particle Polymer Matrix Composite. Journal of Southwest Jiaotong University. 2019;54(4).
18. Mezan SO, Jabbar AH, Hamzah MQ, Tuama AN, Hasan NN, Roslan MS, Agam MA. Synthesis, characterization, and properties of polystyrene/SiO2 nanocomposite via sol-gel process. NANOSCIENCE AND NANOTECHNOLOGY: NANO-SciTech: AIP Publishing; 2019.
19. Tong Z, Mikheikin A, Krasnoslobodtsev A, Lv Z, Lyubchenko YL. Novel polymer linkers for single molecule AFM force spectroscopy. Methods. 2013;60(2):161-168.

20. Hobbs JK, Farrance OE, Kailas L. How atomic force microscopy has contributed to our understanding of polymer crystallization. Polymer. 2009;50(18):4281-4292.

21. Zhou Z, Zheng C, Li S, Zhou X, Liu Z, He Q, et al. AFM nanoindentation detection of the elastic modulus of tongue squamous carcinoma cells with different metastatic potentials. Nanomed Nanotechnol Biol Med. 2013;9(7):864-874.

22. Nguyen-Tri P, Ghassemi P, Carriere P, Nanda S, Assadi AA, Nguyen DD. Recent Applications of Advanced Atomic Force Microscopy in Polymer Science: A Review. Polymers. 2020;12(5):1142.

23. Bao Y, Luo Z, Cui S. Environment-dependent single-chain mechanics of synthetic polymers and biomacromolecules by atomic force microscopy-based single-molecule force spectroscopy and the implications for advanced polymer materials. Chem Soc Rev. 2020;49(9):2799-2827.

24. Garzon-Hernandez S, Garcia-Gonzalez D, Jérusalem A, Arias A. Design of FDM 3D printed polymers: An experimental-modelling methodology for the prediction of mechanical properties. Materials & Design. 2020;188:108414.

25. C AP, R VSS, Ramachandran A, Selvam A. Modeling and Analysis of Surface Roughness Parameters in Drilling of Silk-glass/epoxy Composite. Materiale Plastice. 2022;59(1):78-89.

26. Sapuan SM, Aulia HS, Ilyas RA, Atiqah A, Dele-Afolabi TT, Nurazzi MN, et al. Mechanical Properties of Longitudinal Basalt/Woven-Glass-Fiber-reinforced Unsaturated Polyester-Resin Hybrid Composites. Polymers. 2020;12(10):2211.

27. Bonta DF, Tofan SA, Todor L, Miron M, Talpos CI, Cosroaba RM, et al. In vitro Study on Mechanical Properties of Polyacid-modified Composite Resins (Compomers). Materiale Plastice. 2022;59(1):90-98.

28. Hassan AM, Almomani M, Qasim T, Ghaithan A. Statistical analysis of some mechanical properties of friction stir welded aluminium matrix composite. International Journal of Experimental Design and Process Optimisation. 2012;3(1):91.

29. Radoi AI, Ciuca I, Stanescu MM, Bolcu D, Nicolicescu C, Miritoiu CM, Bogdan M. Studies Regarding Some Mechanical Properties for a Hybrid Resin Used to Build Composites Reinforced with Corn Cob Powder. Materiale Plastice. 2022;59(2):24-31.

30. Rezakalla-Antypas I, Dyachenko AG. Physical and Mechanical Properties Analysis of Wood-waste Composite Panels. Materiale Plastice. 2022;59(2):61-72.

31. Craeye B, De Schutter G, Vuye C, Gerardy I. Cement-waste interactions: Hardening self-compacting mortar exposed to gamma radiation. Prog Nuclear Energy. 2015;83:212-219.